High Efficiency FRET Processes in BODIPY Functionalized Quantum Dot Architectures

Annamaria Panniello,*[a] Mariachiara Trapani,[b] Massimiliano Cordaro,[c] Carlo Nazareno Dibenedetto,[d,a] Raffaele Tommasi,[e] Chiara Ingrosso,[a] Elisabetta Fanizza,[d,a] Roberto Grisorio,[f] Elisabetta Collini,[g] Angela Agostiano,[d,a] Maria Lucia Curri,[d,a] Maria Angela Castriciano,[b] and Marinella Striccoli*[a]

[a] Istituto per i Processi Chimico Fisici del CNR (IPCF-CNR) c/o Dipartimento di Chimica, Università degli Studi di Bari "Aldo Moro" Via Orabona, 4 70126 Bari, Italy

[b] Istituto per lo Studio dei Materiali Nanostrutturati del CNR (ISMN-CNR) c/o Dipartimento di Scienze Chimiche, Biologiche, Farmaceutiche ed Ambientali, Università degli Studi di Messina Viale F. Stagno D'Alcontres31, 98166 Messina, Italy

[c] Dipartimento di Scienze Chimiche, Biologiche, Farmaceutiche ed Ambientali Università degli Studi di MessinaViale F. Stagno D'Alcontres31, 98166 Messina, Italy

[d] Dipartimento Chimica, Università degli Studi di Bari "Aldo Moro" Via Orabona, 4 70126 Bari, Italy

[e] Dipartimento di Scienze Mediche di Base, Neuroscienze e Organi di Senso, Università degli Studi di Bari "Aldo Moro"Piazza G. Cesare, 11 70124 Bari, Italy

[f] Dipartimento di Ingegneria Civile, Ambientale, del Territorio, Edile e di Chimica (DICATECh) Politecnico di Bari, Via Orabona, 4 70126 Bari, Italy

[g] Dipartimento Scienze Chimiche, Università di Padova via Marzolo 1, 35131 Padova, Italy

*Corresponding Authors

E-mail: a.panniello@ba.ipcf.cnr.it; m.striccoli@ba.ipcf.cnr.it

Keywords: BODIPY functionalization • Energy Transfer • FRET QD-Dye • Luminescence Decay Dynamics • Quantum Dots

Abstract: Efficient FRET systems are developed combining colloidal CdSe quantum dots (QDs) donors and BODIPY acceptors. To promote effective energy transfer in FRET architectures, the distance between the organic fluorophore and the QDs needs to be optimized by a careful system engineering. In this context, BODIPY dyes bearing amino-terminated functionalities are used in virtue of the high affinity of amine groups in coordinating the QD surface. A preliminary QD surface treatment with a short amine ligand is performed to favour the interaction with the organic fluorophores in solution. The successful coordination of the dye to the QD surface, accomplishing a short donor-acceptor distance, provides effective energy transfer already in solution, with efficiency of 76%. The efficiency further increases in solid state where the QDs and the dye are deposited as single coordinated units from solution, with a distance between the fluorophores down to 2.2 nm, demonstrating the effectiveness of the coupling strategy.

Introduction

Förster resonance energy transfer (FRET) is one of the key mechanisms taking place between two interacting fluorophores, affecting numerous advanced applications, including (bio)-sensors,[1] energy harvesting[2] and light emitting diodes.[3] The FRET process is an excitation energy transfer occurring via a non-radiative dipole-dipole interaction between an excited donor (D) and an acceptor (A). The FRET efficiency depends on the spectral overlap between the donor fluorescence and the acceptor extinction, on the D-A separation distance, typically ranging from few Å to 10 nm, and on the relative orientation between the transition dipole moments of donor and acceptor.[4] Moreover, according to the classical FRET theory, a high quantum yield (QY) of the donor is required to maximize the process efficiency.[5]

Inorganic quantum dots (QDs) are being increasingly exploited as donors in FRET systems, thanks to their broad absorption spectra, the size-tuneable narrow emission, the high QY and the excellent chemical and photostability. Besides, QDs offer the benefit of minimizing the acceptor direct excitation, as their broad absorption band allows excitation in a large portion of the UV-Vis spectrum, and to tune the FRET efficiency by hosting multiple acceptors per QD.[6] QDs can be also employed as acceptors in FRET systems, as they exhibit large spectral overlap integrals, show high FRET-sensitization rate, since enable interfacing of each QD with multiple donors, and allow to have one donor for multiplexed FRET processes, with simultaneous participation of two or more D-A pairs to the same system.[6]

Several examples are present in the recent literature concerning the fabrication of FRET systems combining QDs-QDs of different sizes or QDs and dyes. A variety of FRET studies performed on thin films made of close-packed CdSe QDs with mixed sizes demonstrate that the smaller QDs behave as exciton donors and the larger ones as acceptors in the ET process.[7] Recently, Hoffman et al. have demonstrated the key role of the QD surface chemistry in the design and engineering of functional devices based on FRET processes.[7b] In the application of the Förster formalism to a homogeneously blended solid-state films composed by two differently sized CdSe QDs, discrepancies between the calculated and the measured FRET parameters have been observed. Such incongruities have been ascribed to several factors as QD shape, transition dipole orientation, enhanced absorption cross-section or dipole-multipole coupling, and highlight the limits of the Förster formalism when applied to solid-state systems.[8]

FRET systems have been obtained by sensitizing the QDs with organic dyes, combining them by means of hydrophobic interactions, or by using an amphiphilic polymeric coating layer able to interdigitate its chains with the pristine ligands.[9] On the other hand, an effective interaction between the donor and acceptor can be achieved by the (bio)conjugation of the QD surface, obtained by directly replacing the pristine ligands with organic dye molecules or by using functional linkers to mediate the conjugation. In the first case, the dye is required to bear chemical groups suitable to bind the QD surface (thiols, amines or carboxylates). In the second case, a bi-functional linker can be used to connect QD and dye, allowing the modulation of the distance between donor and acceptor.

Among the organic dyes, compounds containing rigid aromatic units or macrocyclic structures, such as phthalocyanines and porphyrins, are largely used as FRET acceptors. Indeed, these molecules present a relatively simple synthesis and can be possibly further derivatized to insert specific functional groups able to bind the donor surface.[5] In addition, a proper setting of the number of functional moieties and their arrangement on the dye aromatic ring may lead to the formation of polydentate ligands that are expected to bind more strongly to the QD surface, due to the chelating effect, thus, ultimately, envisaging higher FRET efficiencies.

Few studies report FRET systems based on QD-linker-dye architecture, where the rigidity of the linker plays also a fundamental role in the energy transfer process, enabling a systematic experimental validation of FRET theory.[10]

A coupled D-A FRET system has been developed by covalently binding an ATTO-dye to the CdSe QD surface.[11] QDs-dye coupled systems have been reported as effective pH-responsive sensors, for example for measuring the cellular pH,[12] or for the selective sensing of metal cations.[13] A wealth of examples reports the application of FRET systems relaying on QDs coupled to dye molecules, through the conjugation with the organic shell surrounding the nanoparticles,[10a, 14] or involving the formation of bioconjugates, also via non-specific interactions (electrostatic interactions, hydrogen bonds) with biological molecules, as proteins or oligonucleotides.[15]

Here, the purpose of the work is to fabricate highly efficient FRET systems, in both solution and solid state, coupling colloidal CdSe QDs and BODIPY molecules, properly derivatized with aminostyril groups to allow their direct anchoring at the QD surface.

In particular, monoaminostyryl substituted BODIPY (MASB), with one amino moiety, and diaminostyryl functionalized BODIPY (DASB), a bidentate dye bearing two amino groups, have been selected and synthesized.[16] A preliminary treatment of the QD surface with ethanolamine (EA) has been performed to favour the interaction with the organic fluorophores in solution. While the DASB, due to its high steric hindrance and its poor spectral overlap, provides a limited FRET efficiency (29%), the MASB/QDs hybrid system demonstrates very effective transfer properties already in solution with an efficiency of 76% and a calculated center to center D-A distance of 2.6 nm, consistent with the effective coordination of the dye at the QD surface. The coupling procedure results successful also when the QDs and the organic chromophores are deposited on a substrate as single combined units, with respect to the conventional layer-by-layer approach. Indeed, the FRET efficiency of QDs/DASB and QDs/MASB systems enhances up to 58% and 80%, respectively, thus demonstrating the effectiveness of the coupling strategy even in solid state.

Results and Discussion

To design an efficient FRET system based on BODIPYs successfully coupled to the QD surface, several issues need to be considered. Firstly, QD size should be selected to confer to the donor the emission spectrum well overlapping the absorption of the dye. Then, both the fluorophores need to be dispersed in the same solvent and, finally, the QD surface has to be sterically available for the dye approach and its effective anchorage, to minimize the D-A distance. While QDs prepared by means of hot injection synthesis are generally highly dispersible in poorly polar organic solvents, such as hexane, toluene or chloroform, the aminostyryl substituted BODIPYs are soluble in polar organic solvents, such as methanol or tetrahydrofuran. Therefore, to disperse the chromophores in the same medium, the chemical structure of the BODIPY and/or QD surface chemistry needs to be suitably modified. For this purpose, an exchange of the QD pristine capping layer with a new ligand has been performed. Indeed, ligand exchange represents a simpler and more versatile approach than the modification of the BODIPY chemical structure that would require more demanding synthetic and purification efforts, possibly inducing a substantial alteration of dye optical properties. The new ligand needs to be a bifunctional molecule able to coordinate QDs and, at the same time, expose polar end groups to facilitate their dispersion in polar solvents. In addition, to favour the dye approach at the QD surface, the ligand should be endowed with a short and linear aliphatic chain. In fact, the QD pristine capping layer, composed of long chain amines, phosphines or carboxylic acids, is characterized by a considerable steric hindrance, detrimental for the dye molecule penetration and

anchoring to the QD surface. Then, the new ligand should help thin out the QD surface. However, a capping agent with a short alkyl chain cannot provide the QDs with adequate colloidal stability in solution. On the other hand, the original capping layer is effective in passivating the QD surface, preserving the optical properties, while its complete exchange can lead to a dramatic deterioration of the emission. Therefore, only a partial replacement of the capping layer with the new ligand can conveniently overcome these critical issues.

Here, a two-step procedure has been proposed for the fabrication of the FRET system. Firstly, a preliminary partial capping exchange of the QD surface by using a short chain ligand, namely ethanolamine (EA), has been carried out. Such pre-treatment ensures the dispersion of QDs in a solvent suitable to solubilize also the dye molecules, reducing, at the same time, the steric hindrance of the ligand at QD surface. Then, the second step consisted in the functionalization of the QDs with the dye molecules, by taking advantage of the aminostyril groups available for the coordination to the CdSe surface.

Ligand exchange with EA

EA has been selected as bifunctional ligand to coordinate the QD surface, being characterized by a short alkyl chain (~0.4 nm long), and an amino functionality that has a good affinity with the CdSe QD surface.[17] According to a recent classification,[18] TOPO and HDA are L-type ligands, as possess a lone electron pair, able to coordinate surface metal atoms, while OLEA is an X-type ligand that can donate one electron. Any ligand exchange reaction at the surface of the QDs has to ensure their electro-neutrality. The addition of the short EA ligand can provide, by mass action, the removal of some of the pristine amphiphilic long alkyl chain TOPO and HDA molecules from the QD surface, opening available space in the capping layer, which is advantageous for penetration of new solvent or new molecules.

FT-IR-ATR analysis has been carried out in order to investigate the chemistry at the CdSe QD surface before and after the capping exchange with EA. The FT-IR-ATR measurements of the EA-CdSe QDs (Figure S1 in the SI) clearly demonstrate that EA binds the CdSe QDs through the amino groups, as discussed in detail in the SI. Due to the -OH group of the EA ligand, the CdSe QDs can be, in principle, dispersed in polar solvents. However, the presence of residual pristine OLEA molecules, along with the retention of TOPO and HDA ligands, only provides their sufficient dispersion in a DCM/MeOH 70/30 % v/v mixture. Such a binary mixture, able also to solubilize the BODIPYs, has been used as solvent for the fabrication of the BODIPY/QDs FRET architectures, as reported in the experimental section.

The UV-Vis absorption and PL spectra of the QDs, before and after the ligand exchange, are reported in Figure 1A. The “as synthesized” QDs show the typical absorption profile[19] characterized by a well-defined first excitonic peak, which is also preserved after the organic shell modification with EA (Figure 1A). The tail at long wavelengths in the EA-QD absorption spectrum can be ascribed to Rayleigh light scattering, due to their reduced dispersibility in the binary solvent mixture that induce an aggregation, though limited, of the nanoparticles, with respect to that of the “as synthesized” QDs in hexane.

TEM micrographs and the statistical analyses, acquired on the “as synthesized” and the EA-QDs, indicate that the QDs do not significantly differ in terms of shape, size and size distribution, presenting, in both cases, a mean particle size of 3.3 nm (σ% =6%) (Figure S2 in the SI), without any relevant nanoparticle aggregation upon EA treatment (inset of Figure 1A).

The PL spectra (Figure 1A) show a decrease of the emission intensity of EA- QDs. Figure 1B reports the PL decays of the QDs before and after the EA treatment. The “as synthesized” CdSe QDs

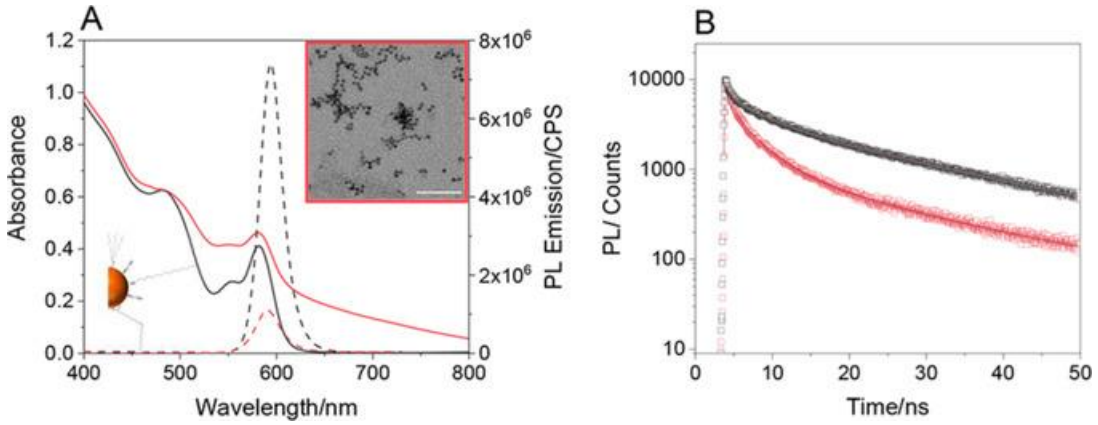

Figure 1. (A) UV-Vis absorption (solid lines) and PL emission (dashed lines) spectra of CdSe QDs capped by pristine (black, hexane solvent) and EA (red, DCM/MeOH solvent) ligands. The inset shows a TEM picture of EA-QDs (scale bar 50 nm). (B) TR-PL decays of the CdSe QDs before (black squares) and after the capping exchange with EA (red squares), detected at the PL peak (λExc=485 nm). The corresponding data fitting are reported as solid lines.

have a multi-exponential fluorescence decay that has been best-fitted by a 3-exponential function with an average lifetime of 18.7±0.5 ns (Table S1 in the SI), in accordance with the literature.[20]

Upon the EA introduction into the organic shell, a substantial shortening of the recombination dynamics is observed, with an average lifetime of 10.6±0.3 ns. Both the variations can be ascribed to the partial deprotection of the QD surface, caused by the limited desorption and displacement of the pristine ligands by the short bifunctional EA molecules whose surface passivation results less efficient. Moreover, the solvent composition and its different polarity also affects the QD emission and the exciton relaxation dynamics.[20a, 21]

FRET systems in solution

Hybrid systems for ET have been fabricated by properly functionalizing the EA-QDs with BODIPYs molecules. Namely, two organic fluorophores, MASB and DASB, have been specifically synthesized to promote the formation of the supramolecular adducts by means the high affinity of the amino group for the QD surface. Furthermore, the DASB, bearing two amino functionalities, is expected to bring the additional advantage of a bidentate coordination to the QD surface, although its higher steric hindrance can be detrimental.

On the other hand, the introduction of substituent groups on BODIPY skeleton at the meso and pyrrolic positions can significantly affect the photophysical properties, and, accordingly, turns into a different FRET behaviour. The MASB and DASB have optical features in the red region of the electromagnetic spectrum,[22] with main absorption peaks at 596 nm and 677 nm, respectively, attributed to the S0→S1 transition[23] and corresponding fluorescence emission bands at 673 nm and 713 nm (Figure S3 in the SI). The functionalization of the EA-QDs with the BODIPYs has been performed according to the procedure reported in the experimental section, using an excess of dye with respect to EA-QDs.

The absorption line-shape of the EA- QDs/MASB system is shown in Figure 2A. The close spectral proximity of the MASB signal to the main excitonic peak of QDs hinders a clear identification of the dye absorption, while the tail at long wavelengths reflects the spectroscopic characteristics of the EA-QDs. However, a faint variation in the spectral position of the main absorption peak of the coupled system (Inset of Figure 3A) suggests a change in the EA-QD. surface chemistry and environment that can be ascribed to the interaction between the two fluorophores.

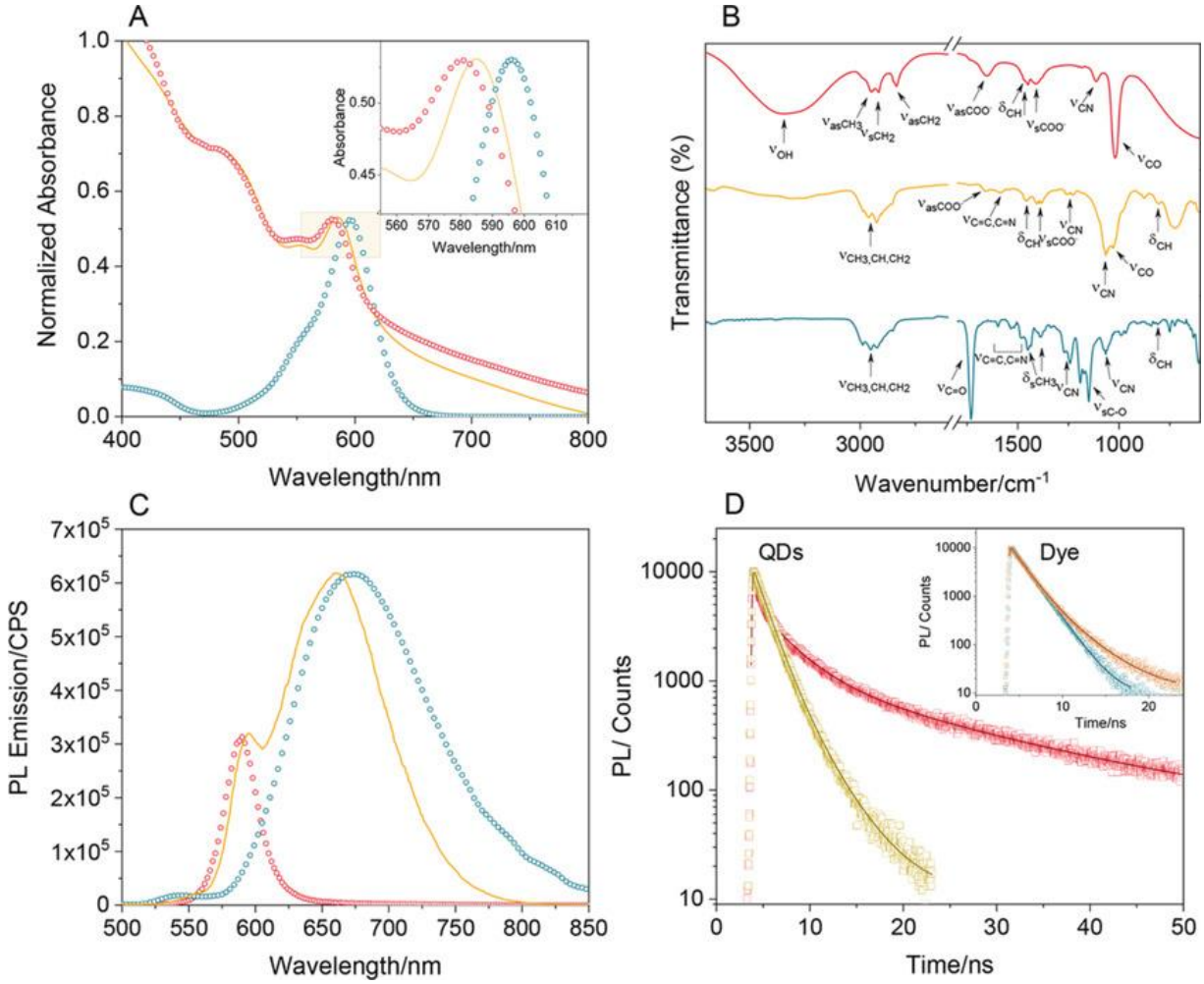

Figure 2. (A) UV-Vis absorption spectra of EA-QDs/MASB system (yellow line), bare EA-QDs (red circles) and MASB (blue circles). In inset: magnification of the absorption peaks. (B) FT-IR-ATR spectra of EA-QDs/MASB system (yellow line), EA-QDs (red line) and MASB (blue line). (C) PL emission spectra of EA-QDs/MASB system (yellow line), EA-QDs (red circles) and MASB (blue circles) (λExc 485 nm). For sake of clarity, the absorption and PL intensities of QDs and MASB are displayed as normalized to the corresponding peaks of the coupled system. (D) TR-PL intensity decays of the EA-QDs (red squares) and EA-QDs/MASB system (yellow squares), detected at the QD emission peak with the corresponding data fitting (solid line). (In inset) Decay profile of the MASB before (blue squares) and after EA-QD functionalization (dark orange squares) (λExc 485 nm)

Figure 2B shows the FT-IR-ATR measurements of EA-QDs/MASB functionalized system (Figure 2B, orange line), neat EA-QDs (Figure 2B, red line) and MASB (Figure 2B, blue line). The comparison of the spectra, which is discussed in detail in the SI, assesses the coordination of the organic chromophore to the QD surface in the hybrid sample, together with the presence of residual EA capping molecules.

The fluorescence line-shape of the EA-QDs/MASB (Figure 2C) clearly shows the characteristic contributes of the QD excitonic emission and of the dye PL peak, respectively, that appear slightly shifted with respect to the spectra of the single components. The shift provides evidence of the interaction taking place between the two chromophores in solution. It is worth to note that the spectra have been obtained by exciting the samples at 485 nm, in the spectral range where the acceptor has a negligible absorption, while the QD extinction coefficient is very intense. In agreement with the results of the UV-Vis, FT-IR and PL measurements, it can be reasonably assumed that the

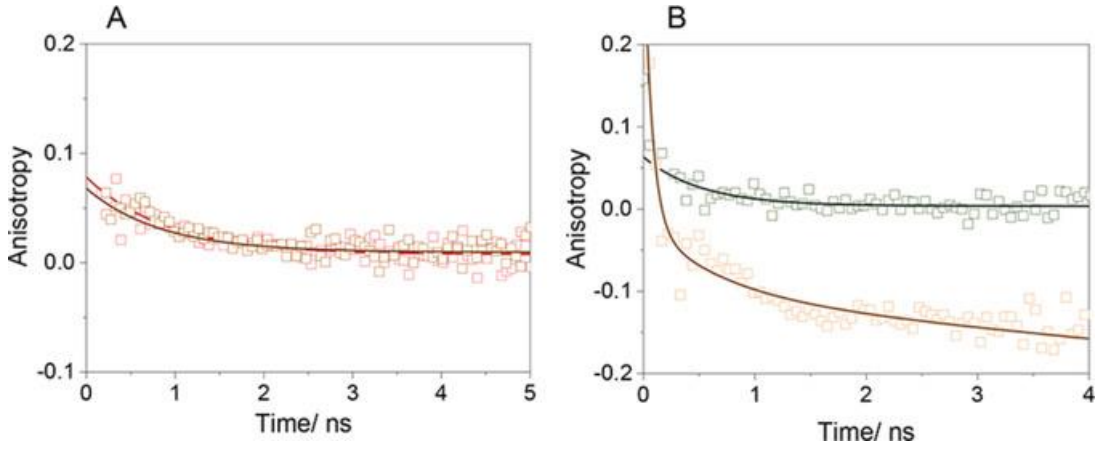

Figure 3. PL Anisotropy decays of: (A) the EA-QDs/DASB system (dark orange squares) and of the neat EA-QDs (red squares), detected at QD emission; (B) the EA-QDs/DASB system (light orange squares) and the DASB molecules in solution (green squares), detected at the dye main emission peak. λExc 390 nm. The corresponding data fittings are represented as solid lines.

MASB coordinates the QDs through supramolecular interactions, involving weak forces between the two fluorophores.

Instead, in case of the EA-QDs/ DASB, the overall line-shape resembles the sum of the single components and no shift in the absorption peak is observed (Figure S5A in the SI). Only a slight broadening of the QD emission on the high-energy side and a red shift of the dye emission peak are detected (Figure S5B in the SI). FT-IR-ATR investigation on the coupled system does not highlight any significant variation in the vibrational spectra of the EA-QDs in the presence of the dye (data not shown). In this case, in spite of the possible, favourable, bidentate binding of DASB, a direct coordination of the dye to the QD surface could not be assessed. Such an evidence can be reasonably ascribed to the higher steric hindrance and to a higher rigidity of DASB with respect to MASB that hamper the approach to the QD surface through the capping layer. However, the DASB and the QDs can interact through FRET mechanisms in solution, if they are sufficiently close to each other.

The distinctive mark of a FRET process between two fluorophores is the quenching of donor emission together with the concomitant enhancement of the acceptor fluorescence, which also reflects in a shorter donor lifetime. The PL decays of the EA-QDs and of the MASB, together with those of the coupled system, are reported in Figure 2D, while the analogous measurements for the DASB system are in Figure S5 C-D of the SI.

The surface functionalization with BODIPYs speeds up the QD average lifetime from 10.6±0.3 ns to 2.53±0.03 ns for MASB and to 7.51±0.01 ns for DASB, respectively (Table S1 in the SI). In addition, the single-exponential PL decay of the BODIPYs is fitted by a bi-exponential function in the coupled system and gets slower in time, passing from 1.75±0.02 ns to 2.06±0.01 ns for MASB. The DASB shows an analogous behavior, indicating the occurrence of a FRET process, although the FT-IR-ATR analysis does not highlight an effective coordination between the fluorophore and the QDs. To further clarify this point and assess the possible formation of supramolecular structures between QDs and DASB, the rotational diffusion of the fluorophores has been investigated by fluorescence anisotropy decay [r(t)], carried out on the EA-QDs/DASB system (Figure 3). The rotational correlation time, detected at the QD excitonic emission, appears unchanged within the limits of the experimental error, by the presence of the dye in solution (Figure 3A), whereas a significant change is observed at the DASB emission (Figure 3B). The anisotropy decay time for the neat DASB is fitted as a single exponential with a rotational correlation time of about 0.5 ns (Figure 3B, green squares), while the hybrid system shows two rotational correlation times, one of about 1.5 ns and the other

longer than 20 ns (Figure 3B, orange squares). Such results suggest that, in the hybrid system, the free rotation of DASB in the solvent is inhibited and the dye molecules move together with the QDs. This can be possibly ascribed to the entrapping of the fluorophore in the organic shell surrounding the QD surface, due to the intercalation of the aminostyryl functional groups of the dye within the long alkyl chain tails of the QD ligands, without, however, the occurrence of an effective surface coordination.

From our experimental findings, the occurrence of a FRET process between the components of the hybrid systems in solution can be reasonably assumed. The FRET efficiency can be calculated by experimental parameters, namely by either the fluorescence peak intensities or the amplitude-weighted average lifetimes obtained by the multi-exponential fitting of the fluorescence decays[24]:

$$E_{FRET} = 1 - \frac{I_{DA}}{I_D} = 1 - \frac{\langle \tau_{DA} \rangle}{\langle \tau_D \rangle} \qquad (1)$$

From the calculations, the FRET efficiency results of 76% for EA-QDs/MASB and only of 29% for DASB hybrid system in solution, respectively. The difference accounts for the stronger spectral overlap between the QD donor and the dye acceptor (Figure 4) and the lower steric hindrance of MASB with respect to DASB. In agreement with the FT-IR measurements, MASB results to more effectively coordinate the QD surface, thus reducing the D-A distance, while DASB amino groups can only reasonably interdigitate the QD ligands.

However, due to the large surface area of the QDs, the interaction of more than one dye molecule on the same QD donor can be expected.[4, 10a, 11, 25]

The direct assessment of the number of dye molecules for each QD, based on the comparison of the extinction coefficient of isolated and coupled components cannot be easily applied here, due to the close overlap of the spectral bands of the fluorophores, particularly for MASB, that does not allow a precise deconvolution of the contributes, and to the possible presence in solution of free dye. A more precise calculation can be obtained by a method based on the Poisson distribution of the dye molecules around the QDs. Such a method,[4, 10a, 25g, 26] allows to determine the average number of acceptors for each QD, based on the fitting of the time resolved decay of the FRET systems with a function that takes into account the Poisson distribution. The calculations, reported in the SI, indicate an average number of about 1.5 molecules of MASB and 1.1 of DASB, respectively, per QD.

To calculate the energy transfer parameters for processes involving QD donors, the classical ET theory is generally well accepted, considering valid the point dipole approximation for D-A distances larger than their respective sizes.[6] The equation expressing the efficiency of the process can be recast as a function of the donor-acceptor distance, *d*, and of R_0, the Förster radius, representing the distance where the energy transfer has a 50% efficiency:

$$E_{FRET} = \frac{NR_0^6}{NR_0^6 + d^6} \qquad (2)$$

where N is the number of acceptors per donor. The spectral overlap between the donor emission and the acceptor absorption contributes to the FRET efficiency, as the Förster radius can be experimentally calculated by:[24]

$$R_0 = \left(\frac{9\ln(10)\kappa^2 \Phi_D J(\lambda)}{128\,\pi^5 N_A\, n^4}\right)^{\frac{1}{6}} \qquad (3)$$

where κ^2 is the orientation factor that can be considered equal to 2/3 for isotropic and dynamically randomly orientated donor and acceptor molecules,[26-27] Φ_D is the fluorescence quantum yield of the donor, N_A is the Avogadro's number, n is the refractive index of the dispersing medium and $J(\lambda)$ is the spectral overlap integral that has been calculated by:[24]

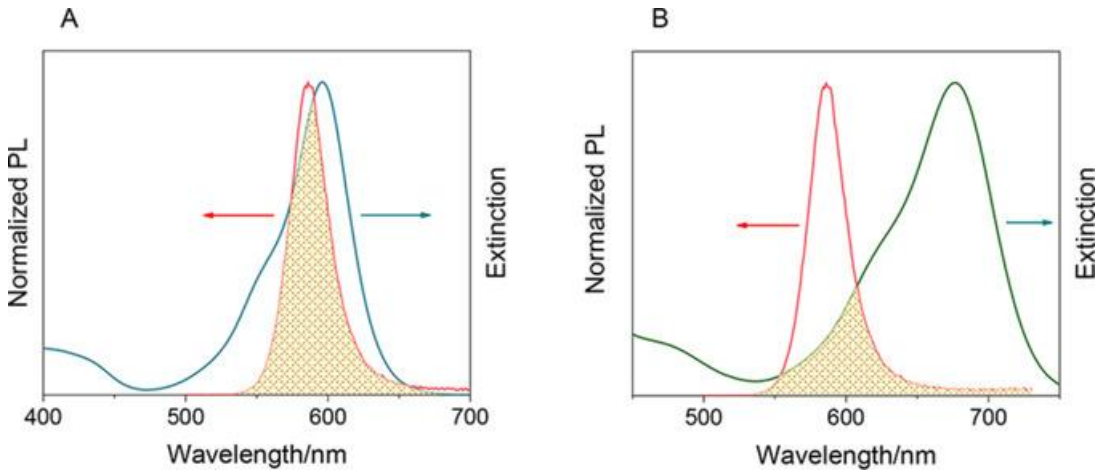

Figure 4. Normalized PL emission spectrum of EA-QDs (red line, left axis) superimposed to the extinction spectrum of (A) MASB (blue line, right axis) and (B) DASB (green line, right axis). The resulting spectral overlap integrals, J(λ), are represented as shaded areas.

$$J(\lambda) = \frac{\int F_D(\lambda)\varepsilon_A(\lambda)\lambda^4 \mathrm{d}\lambda}{\int F_D(\lambda)\mathrm{d}\lambda} \qquad (4)$$

In equation (4), $F_D(\lambda)$ is the donor fluorescence intensity, while $\varepsilon_A(\lambda)$ is the acceptor molar absorption coefficient, both dependent on λ. In order to obtain R_0 values in units of nm, the spectral overlap integral $J(\lambda)$ has been calculated in $M^{-1}\,cm^{-1}\,nm^4$, by using nm and $M^{-1}\,cm^{-1}$ as units for λ and $\varepsilon_A(\lambda)$, respectively, in Equation (4).

Figure 4 shows the overlap integrals $J(\lambda)$ between the PL of the QD donor and the extinction spectra of the dye acceptor and highlights the presence of a strong resonance for MASB (A), significantly weaker for DASB (B). Therefore, it is also expected that fainter the spectral overlap, lower the FRET efficiency. From equation (2) and calculating EFRET by equation (1) and the experimental R_0 values according to Equation (3) and reference[7b], the distance d between the two fluorophores can be obtained, as reported in Table 1.

Table 1. FRET parameters calculated by applying the ET[6] theory for the CdSe QDs coupled to MASB or to DASB, both in solution and in solid-state films.

]	E_{FRET} (%)		R_0 (nm)		d (nm)	
	Solution	*Solid State*	*Solution*	*Solid State*	*Solution*	*Solid State*
EA-QDs/ MASB	76	80[a]	3.2	2.5[a]	2.8	2.2[a]
EA-QDs/ DASB	29	55[b] 58[a]	3.5	3.3[b] 3.1[a]	4.1	3.2[b] 3.0[a]

[a] *"Coupled"* films; [b] *"Bilayer"* films. The "*Coupled*" and "*Bilayer*" labels refer to the procedure used for fabricating the solid D-A systems, as described in the experimental section and schematically summarized in Figure S7A and S8A of the SI. The FRET efficiency has been calculated by using the average lifetimes (Equation (1)).

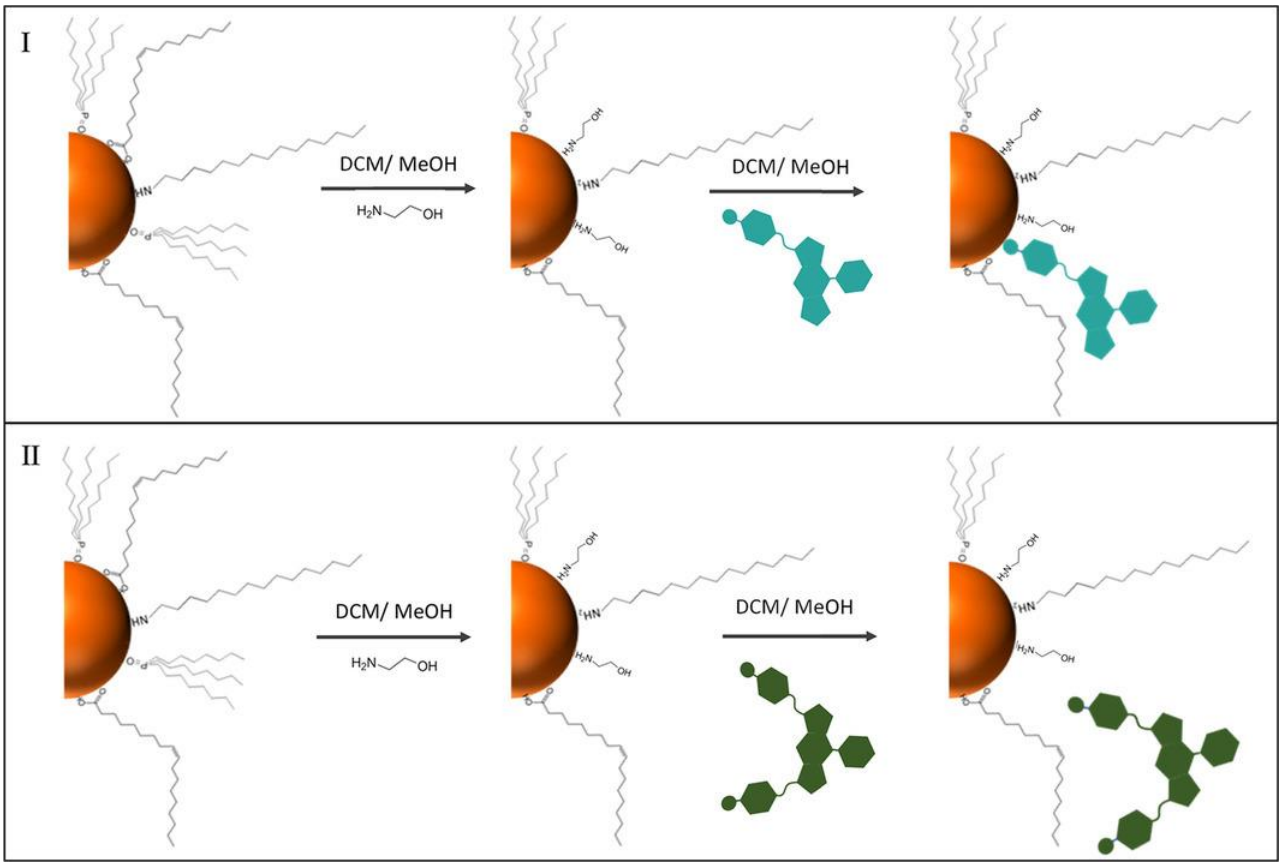

Figure 5. Sketch illustrating the MASB (I, upper panel) and DASB (II, bottom panel) interaction with the QD surface, as emerging from the experimental results.

It is worth noting that, for estimating the distance between the QD and the dye molecule, the PL emission of the donor and the absorption of the acceptor can be reasonably assumed to originate from states positioned at the geometrical centre of chromophores. In agreement with the spectroscopic results, the presence of one aminostyryl group in the fluorophore structure induces a shortening of the calculated centre to centre distance, being 2.8 nm for MASB and 4.1 nm for DASB, respectively. The D-A distance for EA-QDs/MASB system in solution is consistent with the sum of the CdSe QD mean radius (1.7 nm) and the expected mean size of the MASB portion bringing the amino moiety (about 1.2 nm), thus confirming that MASB effectively coordinates the CdSe QD surface, as also indicated by FT-IR-ATR measurements and illustrated in the sketch in Figure 5. Instead, in solution, the estimated d value of 4.1 nm for DASB results larger than the simple sum of the QD mean radius and the expected mean size of the DASB region carrying the amino groups. Here, an accurate evaluation of such a distance needs to take into account the presence of the organic ligand shell formed by the ligand molecules that still partially coordinate the QD surface, which is few Å thick for the EA and up to 2 nm thick for the longer alkyl chain HDA. Therefore, in this case, the calculated value of d, can be rationalized with the possible intercalation of the dye into the alkyl chains of the native ligands for few tenths of nm (Figure 5), as confirmed by the fluorescence anisotropy measurements. Then, we can reasonably assume that, in spite of possible multivalent interaction of the DASB at the QD surface, the lower steric hindrance and the larger spectral overlap of MASB allow for a shorter distance and a higher ET efficiency.

FRET systems in solid state

In view of their application in functional materials and sensing devices, the design of FRET systems with enhanced efficiency[26, 27b] in solid state, where the distance between the fluorophores is further decreased, is required. In literature, several examples report efficient FRET systems based on QDs and/or QDs and organic dye composites, obtained by casting or spin coating techniques.[7b, 7c] Here, to demonstrate the effectiveness of the coupling in ET processes the FRET efficiency of solid-state films obtained depositing the previously coupled QD/dye architecture directly from the solution has been evaluated. Two different preparative methods for the FRET system fabrication as a film onto a quartz substrate have been used: i) a conventional "layer by layer" approach, relaying on depositing, by casting, a layer of QDs followed by the deposition of a layer of acceptor molecules ("bilayer" film) and ii) the direct deposition by drop casting of the EA-QDs/MASB or DASB systems, previously coupled in solution ("coupled" film). In all the investigated cases, spectroscopic investigations show the fluorescence quenching of CdSe QDs and the enhancement of the BODIPYs PL (Figures 6; S7 and S8 in the SI), indicating the occurrence of the FRET process. In the calculation of the FRET efficiency in the solid films, the average fluorescence lifetimes of QDs in solution have been used, according to Kamat and co-authors[7b]. In the case of EA-QDs/MASB coordinated system, a weak improvement of the FRET efficiency has been obtained in the film (80%) with respect to solution (76%) (Table 1). Conversely, when FRET efficiency is calculated for the EA-QDs/DASB system, values of about 55% and 58%, for the "bilayer" and the "coupled" film, respectively result (Table 1). These values have to be compared with the efficiency of the same system in solution, that is only 29%. Such a significant enhancement can be ascribed to an increased proximity between the fluorophores in solid state, due to the absence of solvent. Moreover, the lack of solvent induces a coiling of the longer alkyl chains of the molecules capping the QDs, as they cannot extend their structure, as it would happen in the presence of a "good" solvent. As a result, a thinner shell is expected, and concomitantly, leads to a decrease of the D-A distance.

However, in solid state, possible HOMO FRET transfer phenomena can also occur among the QDs in the close packed films, as the inhomogeneous size distribution of the QDs and their close proximity, together with the exciton diffusion towards quenching sites, strongly affect the intrinsic decay rate.[7a, 28] The calculated HOMO FRET contribution results lower than that of the coupled dye/QD system, while it has a greater influence in the case of DASB, as reported in the SI (Figure S9 and table S2).

The determination of the theoretical separation distance between donor and acceptor can be obtained in solid state by applying the FRET theory, as described above (Equations 2-4). According to [7b], the calculation of R_0 for solid state takes into account a different value of the refractive index experimented by the QDs, determined as a volume-weighted average of the refractive index of CdSe and the organic components, and the change in the overlap integral. In particular, the curves of the FRET efficiency as a function of the D-A distances can be plotted by equation (2), imposing the experimental R_0 value previously obtained.

In Figure 6C, the curves of the FRET efficiency for the EA-QDs/MASB coordinated system in solution and in solid film (solid and dashed line, respectively) are compared to the experimental E_{FRET} values determined by the time resolved measurements (symbols). While in solution a *d* value of 2.8 nm is obtained for MASB coordinated at the QD surface, in solid state the D-A calculated distance decreases down to 2.2 nm, thus suggesting a possible change in the dye molecule geometry and a closer packing occurring in absence of the solvent that reflects in a moderate increase of the FRET efficiency. Furthermore, it has been demonstrated that, when the acceptors are in close proximity to the QD surface, complex interactions with surface states may provide some deviations from the Förster formalism, including aberration in the rigorous calculation of the D-A separation

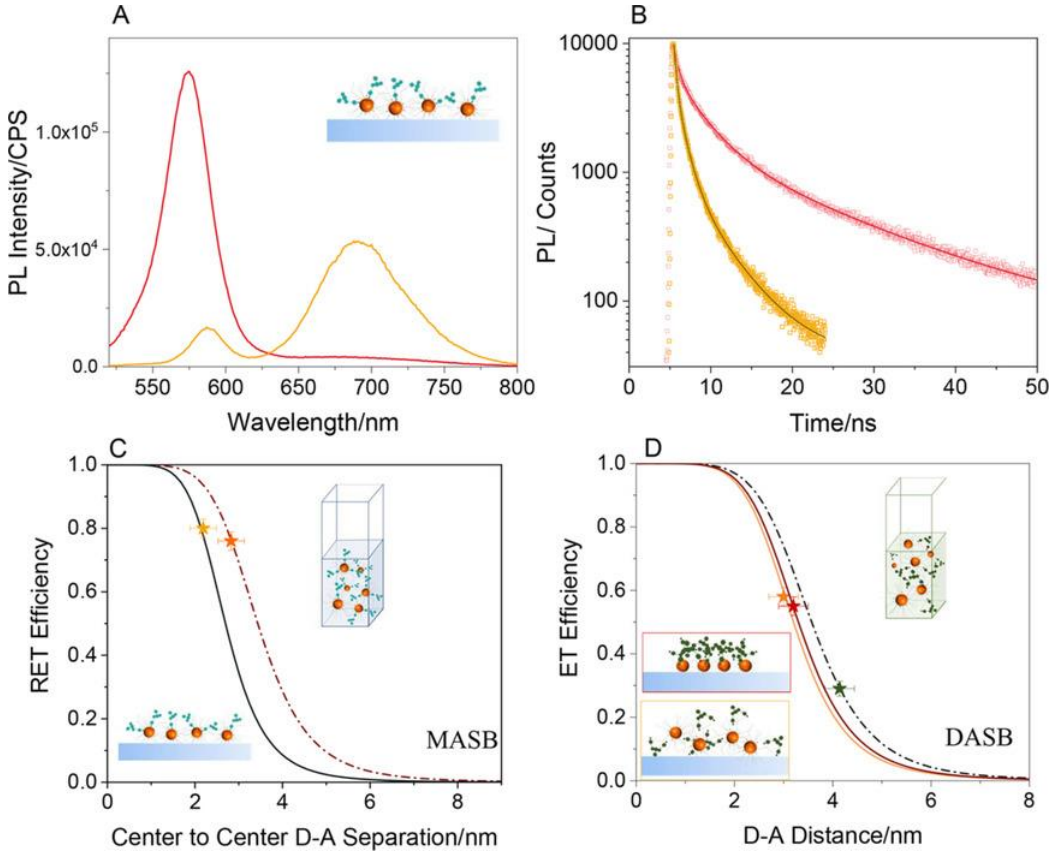

Figure 6. (A) PL spectra of the EA-QDs/MASB coordinated system (yellow line) and of the EA-QDs (red line) deposited on quartz substrates (λExc=485 nm). (B) The corresponding PL decays with data fitting (solid line), in correspondence of the QD emission peak. (C-D) Theoretical ET efficiency as a function of the D-A distance, d, for (C) EA-QDs/MASB system in solid state (blue solid line) and in solution (red dashed line) and for (D) EA-QDs/DASB systems, in the two deposition procedures, namely "coupled" (orange line) and "bilayer" (purple line) and in solution (green dashed line), calculated by Eq. (2). The solid points represent the experimental values

distance.[29] For the QD/DASB systems, the curves of the FRET efficiency in solution and for the *"coupled"* and *"bilayer"* films are reported in Figure 6D. In solid state, the *d* values and the FRET efficiency calculated for the two deposition modes described above, namely for the *"bilayer"* and the *"coupled"* films, differ remarkably from the values measured in solution (Table 1). These results can be justified considering that, regardless the film fabrication procedure, in both cases the absence of the solvent reduces the distance, forcing the fluorophores to be in closer proximity, with a possible deeper penetration of the dye in the organic shell covering the QD surface, thus considerably increasing the FRET efficiency. The slight difference in efficiency and *d* values calculated for the diverse deposition modes still confirms that, even if the DASB does not coordinate the QD surface, the deposition of the two fluorophores as a single unit from solution provides higher FRET efficiency with respect to the layer-by-layer approach.

The overall results demonstrate that the MASB is able to effectively coordinate the QD surface, thus providing a highly efficient FRET architecture, both in solution and in solid state, due to the limited steric hindrance of the dye and the strong spectral overlap of its absorption spectrum with the QD emission.

Beside the wealth of applications that can be envisioned for this system in the field of the FRET-based devices, the very short distance achieved between the donor and the acceptor moieties is highly promising in terms of the investigation of possible coherent effects in the energy transfer process.

Recent experimental and theoretical findings have confirmed the possibility of reliably measuring coherent dynamics processes in the relaxation dynamics of isolated QDs in solutions[16c, 30] or interacting QDs in solid state films.[31] Thus, the QD/MASB hybrids appear as ideal systems to investigate the presence of coherent mechanisms of energy redistribution between the inorganic and the organic moieties in the ultrafast timescales, opening up a completely new niche of possible applications.

Conclusion

An interesting approach, based on the effective coupling between CdSe QDs and BODIPY dyes, has been proposed to realize highly efficient FRET systems both in solution and in solid state. For this purpose, two BODIPY based fluorophores have been designed and synthesized, bearing, respectively, one or two aminostyril functional groups, having a good affinity with the QD surface. A partial exchange of the native QD capping layer with a short alkyl chain bifunctional ligand has been preliminary performed to make QDs dispersible in the same medium of the dyes and, concomitantly, to leave available space at the QD surface, for the dye to approach and anchor. The proper derivatization of the dye with one aminostyril group in MASB has allowed the successful coordination of the dye at the QD surface in solution, minimizing the D-A distance and resulting in high FRET efficiency in solution. Conversely, the DASB demonstrates a limited efficiency due to the higher steric hindrance and the only partial spectral overlapping. The coupling procedures result effective also in solid state, when the hybrid systems are deposited onto substrate as single coupled units. The illustrated strategy can effectively impact the design and preparation of hybrid systems that can find application as FRET sensors both in solution and in solid state. In addition, the very short D-A distance achieved in the coupled systems allows for advanced investigations of possible coherent interactions between chromophores at such close distances in energy transfer processes.

Experimental Section

Materials and experimental methods of the syntheses of CdSe QDs, mono-aminostyryl phenyl BODIPY (MASB) and di-aminostyryl phenyl BODIPY (DASB) are described in detail in the Supporting Information.

CdSe QDs surface functionalization with EA The QD surface functionalization was performed by diluting the as-synthesized QD hexane solution (2×10^{-4} M) in 1 mL of DCM/MeOH solvent mixture (70/30 % v/v), and quickly adding 20 μL (2×10^{-2} mmol) of a DCM/MeOH stock solution of EA ligand (1.1 M). The final EA to pristine ligand-capped CdSe QDs molar ratio was 2×10^{3}. The dispersion was vigorously stirred overnight, and then the CdSe QDs were collected by repeated cycles of centrifugation at 9000 rpm and re-dispersion in the solvent mixture, allowing the removal of the free ligand excess from the solution.

Surface functionalization by MASB and DASB The surface functionalization of CdSe QDs with the BODIPY dyes was performed by adding to 1 mL of EA-CdSe QDs solution (10^{-5} M in DCM/MeOH), 2×10^{-4} mmol of BODIPY dye (MASB or DASB, 5×10^{-3} M), so as to obtain a molar ratio BODIPY to EA-CdSe QDs of 20. The resulting solution was left under vigorous stirring overnight, and then the dye-functionalized CdSe QDs were washed and collected by several cycles of centrifugation at 9000 rpm and re-dispersed in DCM/MeOH 70/30 % v/v.

CdSe QD film fabrication QDs films, used as references, were prepared by simple drop-casting 50 µL of a 2×10^{-6} M of pristine or EA capped QDs dispersion, respectively in hexane and DCM/MeOH, onto properly cleaned quartz substrates. Similarly, the reference MASB and DASB films were fabricated by drop-casting 50 µL of a 2×10^{-6} M dye solution in DCM/MeOH. Bilayer QDs/DASB films were prepared by drop-casting 50 µL of a 2×10^{-6} M dye solution onto a previously deposited layer of pristine CdSe QDs at the same concentration used to prepare the reference sample. Coupled QDs/DASB based films were obtained by drop-casting 50 µL of coupled EA-QD/ DASB systems in DCM/MeOH solution at a concentration of~ 2×10^{-6} M onto cleaned quartz slides. Coupled QDs/MASB films were prepared by drop-casting 50 µL of EA-QD/ MASB functionalized system in DCM/MeOH solution at a concentration of~ 2×10^{-6} M onto cleaned quartz slides.

Spectroscopic and morphologic characterization methods, and details concerning the determination of the average number of dye acceptors for each QD donor and possible contribution of HOMO FRET between QDs are thoroughly described in the Supporting Information.

Supporting information for this article is given at the link https://chemistry-europe.onlinelibrary.wiley.com/action/downloadSupplement?doi=10.1002%2Fchem.202003574&file=chem202003574-sup-0001-misc_information.pdf

Acknowledgements

This work is financially supported by the MIUR PRIN 2015 Project n. 2015XBZ5YA. The INSTM and the EU funded H2020 FET project COPAC (Contract agreement n.766563) are kindly acknowledged.

References

[1] a) I. L. Medintz, A. R. Clapp, H. Mattoussi, E. R. Goldman, B. Fisher, J. M. Mauro, Nature Mater. 2003, 2, 630-638; b) J. Saha, A. Datta Roy, D. Dey, D. Bhattacharjee, S. Arshad Hussain, Materials Today: Proceedings 2018, 5, 2306-2313; c) L.-H. Yang, D. J. Ahn, E. Koo, Mater. Sci. Eng. C-Biomimetic Supramol. Syst. 2016, 69, 625-630; d) T. Doussineau, A. Schulz, A. Lapresta-Fernandez, A. Moro, S. Körsten, S. Trupp, G. J. Mohr, Chem. Eur. J. 2010, 16, 10290-10299.

[2] a) L. Olejko, I. Bald, RSC Advances 2017, 7, 23924-23934; b) A. Gopi, S. Lingamoorthy, S. Soman, K. Yoosaf, R. Haridas, S. Das, J. Phys. Chem. C 2016, 120, 26569-26578; c) A. Samanta, S. Buckhout-White, E. Oh, K. Susumu, I. L. Medintz, Molecular Systems Design & Engineering 2018, 3, 314-327; d) E. Lee, C. Kim, J. Jang, Chem. Eur. J. 2013, 19, 10280-10286.

[3] a) M. Achermann, M. A. Petruska, S. Kos, D. L. Smith, D. D. Koleske, V. I. Klimov, Nature 2004, 429, 642-646; b) S. Wepfer, J. Frohleiks, A. R. Hong, H. S. Jang, G. Bacher, E. Nannen, ACS Appl. Mater. Interfaces 2017, 9, 11224-11230.

[4] M. Mittal, S. Sapra, Chem. Phys. Chem. 2017, 18, 2509-2516.

[5] I. Chambrier, C. Banerjee, S. Remiro-Buenamañana, Y. Chao, A. N. Cammidge, M. Bochmann, Inorg. Chem. 2015, 54, 7368-7380.

[6] W. R. Algar, M. Massey, U. J. Krull, in FRET – Förster Resonance Energy Transfer (Ed.: I. M. a. N. Hildebrandt), Wiley-VCH Verlag GmbH & Co. KGaA, 2013, pp. 475-605.

[7] a) S. A. Crooker, J. A. Hollingsworth, S. Tretiak, V. I. Klimov, Phys. Rev. Lett. 2002, 89, 186802; b) J. B. Hoffman, R. Alam, P. V. Kamat, ACS Energy Letters 2017, 2, 391-396; c) K. Zheng, K. Žídek, M. Abdellah, N. Zhu, P. Chábera, N. Lenngren, Q. Chi, T. Pullerits, J. Am. Chem. Soc. 2014, 136, 6259-6268.

[8] A. J. Mork, M. C. Weidman, F. Prins, W. A. Tisdale, J. Phys. Chem. C 2014, 118, 13920-13928.

[9] a) X. Gao, Y. Cui, R. M. Levenson, L. W. K. Chung, S. Nie, Nature Biotechnology 2004, 22, 969-976; b) T. Pellegrino, L. Manna, S. Kudera, T. Liedl, D. Koktysh, A. L. Rogach, S. Keller, J. Rädler, G. Natile, W. J. Parak, Nano Lett. 2004, 4, 703-707; c) H. Xia, M. Peng, N. Li, L. Liu, Chem. Phys. Lett. 2020, 740, 137085; d) S. R. Inamdar, G. H. Pujar, M. S. Sannaikar, J. Lumin. 2018, 203, 67-73; e) B. Liu, C. Tong, L. Feng, C. Wang, Y. He, C. Lü, Chem. Eur. J. 2014, 20, 2132-2137.

[10] a) G. Beane, K. Boldt, N. Kirkwood, P. Mulvaney, J. Phys. Chem. C 2014, 118, 18079-18086; b) B. Schuler, E. A. Lipman, P. J. Steinbach, M. Kumke, W. A. Eaton, Proc. Natl. Acad. Sci. U. S. A. 2005, 102, 2754-2759; c) E. Dolghih, W. Ortiz, S. Kim, B. P. Krueger, J. L. Krause, A. E. Roitberg, J. Phys. Chem. A 2009, 113, 4639-4646.

[11] Z. Hua, Q. Xu, X. Huang, C. Zhang, X. Wang, M. Xiao, ACS Nano 2014, 8, 7060-7066.

[12] a) I. L. Medintz, M. H. Stewart, S. A. Trammell, K. Susumu, J. B. Delehanty, B. C. Mei, J. S. Melinger, J. B. Blanco-Canosa, P. E. Dawson, H. Mattoussi, Nature Mater. 2010, 9, 676-684; b) K. Susumu, L. D. Field, E. Oh, M. Hunt, J. B. Delehanty, V. Palomo, P. E. Dawson, A. L. Huston, I. L. Medintz, Chem. Mater. 2017, 29, 7330-7344; c) R. Tang, H. Lee, S. Achilefu, J. Am. Chem. Soc. 2012, 134, 4545-4548; d) A. Shamirian, H. Samareh Afsari, D. Wu, L. W. Miller, P. T. Snee, Anal. Chem. 2016, 88, 6050-6056; e) P. Wu, X. Hou, J.-J. Xu, H.-Y. Chen, Nanoscale 2016, 8, 8427-8442.

[13] a) B. Hu, L.-L. Hu, M.-L. Chen, J.-H. Wang, Biosensors and Bioelectronics 2013, 49, 499-505; b) L. Wu, Q.-S. Guo, Y.-Q. Liu, Q.-J. Sun, Anal. Chem. 2015, 87, 5318-5323; c) A. I. Zamaleeva, M. Collot, E. Bahembera, C. Tisseyre, P. Rostaing, A. V. Yakovlev, M. Oheim, M. de Waard, J.-M. Mallet, A. Feltz, Nano Lett. 2014, 14, 2994-3001.

[14] a) X. Wu, H. Liu, J. Liu, K. N. Haley, J. A. Treadway, J. P. Larson, N. Ge, F. Peale, M. P. Bruchez, Nature Biotechnology 2003, 21, 41-46; b) M. Hardzei, M. Artemyev, M. Molinari, M. Troyon, A. Sukhanova, I. Nabiev, ChemPhysChem 2012, 13, 330-335; c) A. M. Funston, J. J. Jasieniak, P. Mulvaney, Adv. Mater. 2008, 20, 4274-4280.

[15] a) H. Mattoussi, J. M. Mauro, E. R. Goldman, G. P. Anderson, V. C. Sundar, F. V. Mikulec, M. G. Bawendi, J. Am. Chem. Soc. 2000, 122, 12142-12150; b) L. Mattera, S. Bhuckory, K. D. Wegner, X. Qiu, F. Agnese, C. Lincheneau, T. Senden, D. Djurado, L. J. Charbonnière, N. Hildebrandt, P. Reiss, Nanoscale 2016, 8, 11275-11283; c) H. Zhang, D. Zhou, Chem. Commun. 2012, 48, 5097-5099; d) G. Jiang, A. S. Susha, A. A. Lutich, F. D. Stefani, J. Feldmann, A. L. Rogach, ACS Nano 2009, 3, 4127-4131.

[16] a) D. Wang, Y. Shiraishi, T. Hirai, Tetrahedron Letters - TETRAHEDRON LETT 2010, 51, 2545-2549; b) L. Bolzonello, A. Polo, A. Volpato, E. Meneghin, M. Cordaro, M. Trapani, M. Fortino, A. Pedone, M. A. Castriciano, E. Collini, J. Phys. Chem. Lett. 2018, 9, 1079-1085; c) E. Collini, H. Gattuso, L. Bolzonello, A. Casotto, A. Volpato, C. N. Dibenedetto, E. Fanizza, M. Striccoli, F. Remacle, J. Phys. Chem. C 2019, 123, 31286-31293.

[17] a) M. A. Boles, D. Ling, T. Hyeon, D. V. Talapin, Nature Mater. 2016, 15, 141-153; b) C. Bullen, P. Mulvaney, Langmuir 2006, 22, 3007-3013; c) J. K. Cooper, A. M. Franco, S. Gul, C. Corrado, J. Z. Zhang, Langmuir 2011, 27, 8486-8493; d) L. S. Li, N. Pradhan, Y. Wang, X. Peng, Nano Lett. 2004, 4, 2261-2264; e) P. Schapotschnikow, B. Hommersom, T. J. H. Vlugt, J. Phys. Chem. C 2009, 113, 12690-12698.

[18] N. C. Anderson, M. P. Hendricks, J. J. Choi, J. S. Owen, J. Am. Chem. Soc. 2013, 135, 18536-18548.

[19] C. N. Dibenedetto, E. Fanizza, R. Brescia, Y. Kolodny, S. Remennik, A. Panniello, N. Depalo, S. Yochelis, R. Comparelli, A. Agostiano, M. L. Curri, Y. Paltiel, M. Striccoli, Nano Research 2020.

[20] a) A. Panniello, C. Ingrosso, P. Coupillaud, M. Tamborra, E. Binetti, M. L. Curri, A. Agostiano, D. Taton, M. Striccoli, Materials 2014, 7, 591-610; b) M. Jones, S. S. Lo, G. D. Scholes, J. Phys. Chem. C 2009, 113, 18632-18642; c) M. Jones, G. D. Scholes, J. Mater. Chem. 2010, 20, 3533-3538.

[21] E. D. Goodwin, B. T. Diroll, S. J. Oh, T. Paik, C. B. Murray, C. R. Kagan, J. Phys. Chem. C 2014, 118, 27097-27105.

[22] H. Lu, J. Mack, Y. Yang, Z. Shen, Chem. Soc. Rev. 2014, 43, 4778-4823.

[23] a) A. C. Benniston, G. Copley, Phys. Chem. Chem. Phys. 2009, 11, 4124-4131; b) A. Loudet, K. Burgess, Chem. Rev. 2007, 107, 4891-4932.

[24] W. R. Algar, H. Kim, I. L. Medintz, N. Hildebrandt, Coord. Chem. Rev. 2014, 263-264, 65-85.

[25] a) V. J. Bailey, B. P. Keeley, Y. Zhang, Y.-P. Ho, H. Easwaran, M. V. Brock, K. L. Pelosky, H. E. Carraway, S. B. Baylin, J. G. Herman, T.-H. Wang ChemBioChem 2010, 11, 71-74; b) G. Bunt, F. S. Wouters, Biophysical Reviews 2017, 9, 119-129; c) E. M. Conroy, J. J. Li, H. Kim, W. R. Algar, J. Phys. Chem. C 2016, 120, 17817-17828; d) Á. I. Fábián, T. Rente, J. Szöllősi, L. Mátyus, A. Jenei, ChemPhysChem 2010, 11, 3713-3721; e) P. L. T. M. Frederix, E. L. de Beer, W. Hamelink, H. C. Gerritsen, J. Phys. Chem. B 2002, 106, 6793-6801; f) C.-c. Li, W.-x. Liu, J. Hu, C.-y. Zhang, Chemical Science 2019, 10, 8675-8684; g) U. Kaiser, D. Jimenez de Aberasturi, M. Vázquez-González, C. Carrillo-Carrion, T. Niebling, W. J. Parak, W. Heimbrodt, J. Appl. Phys. 2015, 117, 024701.

[26] I. L. Medintz, H. Mattoussi, Phys. Chem. Chem. Phys. 2009, 11, 17-45.

[27] a) A. R. Clapp, I. L. Medintz, J. M. Mauro, B. R. Fisher, M. G. Bawendi, H. Mattoussi, J. Am. Chem. Soc. 2004, 126, 301-310; b) F. K. Chou, M. A. Dennis, Sensors 2015, 15.

[28] a) A. Panniello, M. Corricelli, R. Comparelli, M. L. Curri, A. Agostiano, R. Tommasi, M. Striccoli, Nanoscience and Nanotechnology Letters 2015, 7, 67-73; b) Y. Shirasaki, G. J. Supran, M. G. Bawendi, V. Bulović, Nature Photonics 2013, 7, 13-23; c) M. Kozub, Ł. Pawicki, P. Machnikowski, Phys. Rev. B 2012, 86, 121305.

[29] S. Dayal, C. Burda, J. Am. Chem. Soc. 2007, 129, 7977-7981.

[30] E. Cassette, J. C. Dean, G. D. Scholes, Small 2016, 12, 2234-2244.

[31] E. Cohen, P. Komm, N. Rosenthal-Strauss, J. Dehnel, E. Lifshitz, S. Yochelis, R. D. Levine, F. Remacle, B. Fresch, G. Marcus, Y. Paltiel, J. Phys. Chem. C 2018, 122, 5753-5758.